The Mock LISA Data Challenges: from Challenge 1B to Challenge 3

The *Mock LISA Data Challenge Task Force*: Stanislav Babak[1], John G. Baker[2], Matthew J. Benacquista[3], Neil J. Cornish[4], Jeff Crowder[5], Shane L. Larson[6], Eric Plagnol[7], Edward K. Porter[1], Michele Vallisneri[5,8], Alberto Vecchio[9,10] and the *Challenge-1B participants*: Keith Arnaud[2], Leor Barack[11], Arkadiusz Błaut[12], Curt Cutler[5,8], Stephen Fairhurst[13], Jonathan Gair[14,1], Xuefei Gong[15], Ian Harry[13], Deepak Khurana[16], Andrzej Królak[17], Ilya Mandel[8,10], Reinhard Prix[18], B. S. Sathyaprakash[13], Pavlin Savov[8], Yu Shang[15], Miquel Trias[19], John Veitch[9], Yan Wang[20], Linqing Wen[1,8,21], John T. Whelan[1]

[1] Max-Planck-Institut für Gravitationsphysik (Albert-Einstein-Institut), Am Mühlenberg 1, D-14476 Golm bei Potsdam, Germany
[2] Gravitational Astrophysics Lab., NASA Goddard Space Flight Center, 8800 Greenbelt Rd., Greenbelt, MD 20771, USA
[3] Center for Gravitational Wave Astronomy, Univ. of Texas at Brownsville, Brownsville, TX 78520, USA
[4] Dept. of Physics, Montana State Univ., Bozeman, MT 59717, USA
[5] Jet Propulsion Laboratory, California Inst. of Technology, Pasadena, CA 91109, USA
[6] Dept. of Physics, Weber State Univ., 2508 University Circle, Ogden, UT 84408, USA
[7] APC, UMR 7164, Univ. Paris 7 Denis Diderot, 10, rue Alice Domon et Leonie Duquet, 75025 Paris Cedex 13, France
[8] Theoretical Astrophysics, California Inst. of Technology, Pasadena, CA 91125
[9] School of Physics and Astronomy, Univ. of Birmingham, Edgbaston, Birmingham B152TT, UK
[10] Dept. of Physics and Astronomy, Northwestern Univ., Evanston, IL, USA
[11] School of Mathematics, Univ. of Southampton, Southampton, SO171BJ, UK
[12] Inst. of Theoretical Physics, Univ. of Wrocław, Wrocław, Poland
[13] School of Physics and Astronomy, Cardiff Univ., 5, The Parade, Cardiff, CF243YB, UK
[14] Inst. of Astronomy, Univ. of Cambridge, Madingley Rd., Cambridge, CB30HA, UK
[15] Inst. of Appl. Math, Acad. of Math. and System Sci., Chinese Academy of Sciences, 55 Zhongguancun Donglu, Beijing, 100080, China
[16] Indian Institute of Technology, Kharagpur, India
[17] Inst. of Mathematics, Polish Academy of Sciences, Warsaw, Poland
[18] Max-Planck-Institut für Gravitationsphysik (Albert-Einstein-Institut), D-30167 Hannover, Germany
[19] Dept. de Física, Universitat de les Illes Balears, Cra. Valldemossa km. 7.5, E-07122 Palma de Mallorca, Spain
[20] Dept. of Astronomy, Nanjing Univ., 22 Hankou Road, Nanjing, 210093, China
[21] School of Physics, M013, Univ. of Western Australia, 35 Stirling Highway, Crawley, WA 6009, Australia

E-mail: `Michele.Vallisneri@jpl.nasa.gov`

Abstract. The Mock LISA Data Challenges are a program to demonstrate LISA data-analysis capabilities and to encourage their development. Each round of challenges consists of several data sets containing simulated instrument noise and gravitational waves from sources of undisclosed parameters. Participants are asked to analyze the data sets and report the maximum information about the source parameters. The challenges are being released in rounds of increasing complexity and realism: here we present the results of Challenge 1B [issued... new groups...] and we describe Challenge 3 [which includes...].

PACS numbers: 04.80.Nn, 95.55.Ym

1. Introduction

Gravitational radiation from millions of sources, most of which in our Galaxy, but many populating the low-to-high redshift Universe, is expected to be recorded by the Laser Interferometer Space Antenna (LISA), an ESA/NASA mission to survey the gravitational wave (GW) sky in the frequency window $\sim 10^{-5}$–10^{-1} Hz[1]. Such variety of signals, overlapping in time and frequency space (to the limit of confusion in parts of the frequency range) poses a number of interesting new challenges in data analysis, whose solution is essential for the science exploitation of such a complex and innovative instrument.

The LISA International Science Team (LIST) initiated in 2005 a programme known as Mock LISA Data Challenges (MLDCs) with the goal of understanding at the conceptual and quantitative level the intricacies of LISA data analysis, of demonstrating LISA's observational capabilities and of beginning the development of data analysis algorithms, pipelines and prototype infrastructure: a Task Force chartered by the LIST issues periodically data sets containing synthetic noise and GW signals from sources of undisclosed parameters and challenge participants return detection candidates and parameter estimates that are then compared with those originally injected in the data sets.

Three rounds of MLDCs, spanning approximately six months each, have been completed so far. Challenge 1 [2, 3] focused on establishing the basic techniques to observe Galactic (intrinsically monochromatic) binaries, isolated or moderately interfering, and the in-spiral phase of bright, isolated non-spinning massive black hole (MBH) binary systems. Challenge 2 [4] provided three considerably more complex subchallanges: a data set containing approximately 26 million (monochromatic) Galactic binaries drawn from a synthetic population; a data set with the same (though generated with different random seeds) Galactic binary population, with superimposed an unknown number (between 4 and 6) of in-spirals from nonspinning-MBH binaries with a range (between 10 and 2000) of single-interferometer optimal signal-to-noise ratios (SNRs) and coalescence times and five extreme-mass-ratio inspirals (EMRI) with optimal SNRs between 30 and 100. Lastly, five data sets each containing a single EMRI superimposed to Gaussian and stationary instrumental noise, with optimal SNRs between 40 and 110.

The very steep increase in complexity introduced by Challenge 2 over a short time-scale and the need to consolidate analysis techniques before moving to even more taxing challenges motivated a second round of Challenge 1-type MLDCs. In particular, analysis pipelines for EMRIs, already included in Challenge 2, were particularly immature due to the complexity of the problem. These concepts inspired Challenge 1B, with data sets distributed in late Summer 2007 and results submitted

in December 2007. Challenge 1B is in essence a fresh release of Challenge 1 data sets with the addition of data sets containing a single EMRI (with a range of SNRs) embedded in Gaussian and stationary instrumental noise. Ten collaborations took part to Challenge 1B. Highlights from this round include the range of techniques and groups that successfully recovered the signals from galactic binaries and MBH binary systems and the first convincing demonstration of the detection of EMRIs. An additional interesting though un-planned outcome of Challenge 1B was the lack of detection of any signal from a particular data set, where indeed gravitational waves were (unintentionally) generated with an SNR too low to allow their observation. Results from Challenge 1B are presented and discussed in Section 2 and additional details are given in Refs XXX[**include GWDAW proceedings where available**].

Challenge 3 data sets have just been released and results are due in December 2008. They introduce a number of innovations, including two new classes of signals – short-lived bursts and isotropic stochastic backgrounds – and more realistic galactic binary and MBH binary waveforms and LISA noise models. They also see for the first time the release of individual phase-meter channels for selected data sets. Section 3 is devoted to the descriptions of Challenge 3 innovations.

2. Report on Challenge 1B

Challenge 1B focuses on three classes of sources treated independently: (monochromatic) galactic binaries, massive black hole binaries and extreme mass ratio inspirals. The results submitted by the participants were assessed still using the simple criteria considered in previous rounds [3, 5] whereby the parameters and waveform from the key file (corresponding to the true signal included in the data set) were compared to those recovered, using as figures of merit the *best recovered* SNR

$$\mathrm{SNR}_{\mathrm{best}} = \frac{(A_{\mathrm{true}}|A_{\mathrm{best}}) + (E_{\mathrm{true}}|E_{\mathrm{best}})}{\sqrt{(A_{\mathrm{best}}|A_{\mathrm{best}}) + (E_{\mathrm{best}}|E_{\mathrm{best}})}}\,, \tag{1}$$

the *correlation*

$$C = \frac{(h_{\mathrm{key}}|h_{\mathrm{rec}})}{\sqrt{(h_{\mathrm{key}}|h_{\mathrm{key}})\,(h_{\mathrm{rec}}|h_{\mathrm{rec}})}}\,, \tag{2}$$

of the true waveform h_{key} with the recovered one h_{rec}, and the simple difference

$$\Delta\lambda = \lambda_{\mathrm{key}} - \lambda_{\mathrm{rec}}\,. \tag{3}$$

between the true parameter in the key file λ_{key} and the "best fit" of the recovered parameter h_{rec}. In the previous equations, $(.|.)$ stands for the usual inner product and A and E denote the two noise-orthogonal TDI channels.

2.1. Galactic binaries: Challenges 1B.1.X

Seven different Challenge 1B.1.X data sets contained signals from monochromatic binaries in a variety of combinations. Seven parameters are required to fully characterize each source: the amplitude $\mathcal{A}$, the (constant) frequency f, the sky location θ, ϕ, the inclination angle ι, the polarization angle ψ, and the initial phase ϕ_0. Five groups – members of the Goddard Space Flight Center (GSFC), a group from the Institute of Mathematics of the Polish Academy of Science and the Institute of Theoretical Physics at the University of Wrocław (IMPAN), members of the Max Planck Institute for Gravitational Physics, the Albert Einstein Institute

(AEI), a collaboration of scientists from the Institute of Applied Mathematics of the Chinese Academy of Sciences and the Department of Astronomy of Nanjing University (MCMNJU) and members of the Universitat de les Illes Balears and the University of Birmingham (UIBBham) – submitted entries for this class of Challenges, though many groups concentrated only on selected data sets and only AEI provided entries for every challenge.

A fair range of techniques was considered. They broadly belong to the same classes adopted in the past for similar MLDCs, see Refs. [3, 5] and references therein. An healthy spectrum of techniques has therefore been identified and has begun to consolidate for this class of signals, but new implementations and different technical solutions are being pursued. GSFC used the X-Ray Spectral Fitting Package (XSPEC) [6] to fit templates to the energy spectra. The package includes a Levenberg-Marquardt optimization algorithm which was used to obtain an initial guess for the source parameters. A Markov Chain Monte Carlo (MCMC) routine, also available in XSPEC, was then used to arrive at the best fit parameters for the sources. IMPAN used a grid-based search featuring a constraint optimal hypercube lattice and matched filtering; the $\mathcal{F}$-statistic [7] was employed to reduced the search space from 7 to 3 parameters. A similar technique was adopted by AEI, and a more complete description of the method is found in [8], though the current modeling of the waveform has been updated to the rigid adiabatic approximation instead of using the long-wavelength limit. MCMNJU, used a genetic algorithm featuring the $\mathcal{F}$-statistic to determine the source parameters, and UIBBham used a MCMC approach, described in more detail in [9].

Three data sets, Challenges 1B.1.1a-c, contained a single monochromatic binary – the main difference between the data sets was the source's frequency – with SNR $\approx 13 - 25$. Table 1 summarises the values of the correlations, see Eq. (2) for each challenge entry. As some of the entries had close fits to the intrinsic parameters (f, θ, and ϕ), but had issues matching the remaining (extrinsic) parameters, these parameters were recalculated using the $\mathcal{F}$-statistic [7]. Results for these recalculated parameters are also provided. Table 2 provides the deviations of the parameter values from the values in the key files of Challenges 1B.1.1a-c. Figure 1 shows how the various groups succeeded in extracting the sky position of the source in Challenge 1b.1.1a.

The Challenge 1b.1.2 data set contained 25 "verification" binaries, defined as sources for which frequency and sky location are exactly known. This simulates the search for signals from galactic binaries that are already known to exist. In fact, five of these binaries are taken from a list of known binaries available on Gijs Nelemans' website [10], while the remaining twenty were simulated binaries. Table 3 contains the global SNRs and correlations between all sources characterized by the parameters in the key file and the sources recovered by the three groups that participated in this challenge. As in Challenges 1B.1.1a-c the issue with the extrinsic parameters caused the correlations to be less than ideal. However, as the intrinsic parameters were provided to the participants an $\mathcal{F}$-statistic calculations were not performed.

The data set for Challenge 1b.1.3 contained the signals from 20 unknown binaries distributed across the LISA band and therefore well separated in frequency space. Unfortunately, there was an issue with the generation of the signals that caused their SNRs to be too small for detection (all were below 1). As a silver lining to this cloud, none of the participating groups responding to this challenge reported a positive detection, providing therefore a meaningful consistency test of the performance of the algorithms.

Table 1. The performance of challenge entries on the single galactic binary challenges as calculated using SNR, and C. Data in which the extrinsic parameters were corrected using the $\mathcal{F}$-statistic are denoted with an asterisk (*); numbers are not reported where the frequency is well off, and the $\mathcal{F}$-statistic is only fitting to noise.

Group	SNR	C	SNR	C	SNR	C
	Challenge 1b.1.1a ($\mathrm{SNR_{key}} = 13.819$)		Challenge 1b.1.1b ($\mathrm{SNR_{key}} = 24.629$)		Challenge 1b.1.1c ($\mathrm{SNR_{key}} = 15.237$)	
AEI	20.435	0.108	18.652	0.922	1.949	-0.190
AEI*	14.199	0.984	23.266	0.996	14.770	0.989
GSFC	13.805	0.992	20.310	0.807	4.827	-0.138
GSFC*			20.987	0.814		
IMPAN	14.427	0.988	25.235	0.981	16.465	0.925
IMPAN*			23.152	0.997	14.194	0.946
MCMNJU	13.524	0.952	22.641	0.906	6.830	0.033
MCMNJU*	14.193	0.996	23.270	0.994		
UIBBham	13.577	0.992	23.479	0.996		

Table 2. The performance of challenge entries on the single galactic binary challenges as calculated using recovered parameter differences. Data in which the extrinsic parameters were corrected using the $\mathcal{F}$-statistic are denoted with an asterisk (*).

Group	$\Delta\theta$	$\Delta\phi$	Δf (nHz)	$\Delta\psi$	$\Delta\iota$	$\Delta\varphi$	$\Delta\mathcal{A}(\times 10^{-23})$
Challenge 1b.1.1a							
AEI	0.0318	-0.120	-2.43	0.217	-0.454	1.17	1.22
AEI*	0.0318	-0.120	-2.43	0.700	0.215	-1.23	1.18
GSFC	0.00412	-0.0715	-1.81	0.708	0.252	1.33	1.20
IMPAN	0.0311	0.0185	2.13	0.454	0.212	-1.06	1.25
MCMNJU	0.0170	-0.0424	-0.534	0.662	0.426	-1.57	2.34
MCMNJU*	0.0170	-0.0424	-0.534	0.746	0.248	-1.44	1.37
UIBBham	-0.00540	-0.0790	-1.51	0.708	0.173	-1.32	0.647
Challenge 1b.1.1b							
AEI	0.0558	-0.00899	0.946	-1.05	0.283	1.63	-0.0664
AEI*	0.0558	-0.00899	0.946	-0.761	0.0776	1.46	0.00307
GSFC	0.462	0.0606	-30.9	2.56	0.182	0.516	-0.0245
GSFC*	0.462	0.0606	-30.9	-0.534	0.198	0.624	0.0665
IMPAN	-0.0203	0.000708	0.852	0.333	0.339	-0.603	0.713
MCMNJU	0.0670	-0.00627	2.069530	-0.732	-0.0643	0.844	-0.223
MCMNJU*	0.0670	-0.00627	2.069530	-0.739	0.0633	1.30	-0.0165
UIBBham	0.0436	-0.00817	1.777530	-0.636	0.0428	1.13	-0.0293
Challenge 1b.1.1c							
AEI	0.0261	0.00530	1.84	-0.499	-1.12	3.02	0.124
AEI*	0.0261	0.00530	1.84	0.0410	-0.0937	-0.123	0.106
GSFC	0.452	-1.48	140	1.82	-0.471	-0.663	-0.695
IMPAN	0.0158	0.0248	3.72	-1.51	-0.197	2.68	0.478
IMPAN*	0.0158	0.0248	3.72	-0.0287	-0.113	0.356	0.0792
MCMNJU	0.555	-0.368	359	-1.59	-0.250	-0.943	-0.532

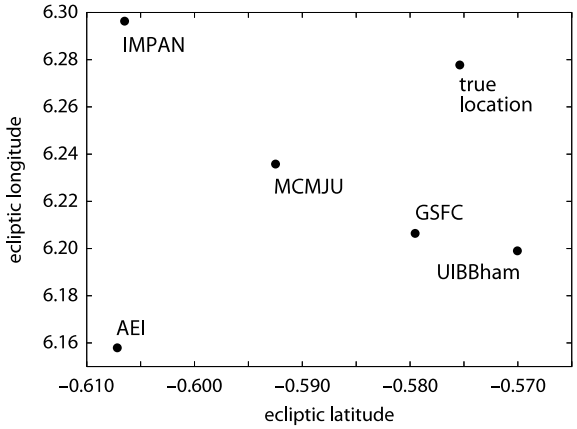

Figure 1. Plot of the sky position for the source from the key file, for Challenge 1b.1.1a, and the recovered sky position for each of the entries.

Table 3. The performance of challenge entries on the verification binaries challenge as calculated using SNR, and C.

Group	SNR	C	# Recovered
Challenge 1b.1.2 ($\mathrm{SNR}_{\mathrm{key}} = 634.918$, 25 Sources)			
AEI	891.677	-0.822	25
GSFC	807.012	0.006	25
MCMNJU	603.805	0.267	25

Challenge 1b.1.4 was a test of the search algorithms in the presence of mild source confusion. Fifty-one sources were spread across a 15μHz band starting at 3 mHz, with an average source density of 0.108 sources per frequency bin. Challenge 1b.1.5 tested the algorithms in the presence of a higher level of source confusion, comparable to that actually produced by our Galaxy during the LISA mission: forty-four sources were spread across a 3μHz band centered on 3mHz; a source density of 0.465 sources per frequency bin. The presence of multiple sources in the data streams of these challenges introduces the possibility of the search algorithms missing sources (false negatives) as well as returning detections when no source is actually present (false positives). To determine the presence of false positives we first matched the frequencies of the recovered sources and those from the key file to within one frequency bin (1/year) of each other. If the correlation between the pair was less than 0.7 (after correcting with the $\mathcal{F}$-statistic) the recovered source was considered a false positive. The two measures for the matches in these challenges, as in Challenge 1B.1.2, are the SNR and correlation. Again, we use the combined signal from all recovered sources compared to the signal from the sources in the key file. Tables **??** and 5 give the results of the two entries to Challenge 1b.1.4 and the single entry to Challenge 1B.1.5. Figure 2 shows plots the MLDC signal from the sources in Challenge 1B.1.4 and the residuals after subtracting the signal from the sources entered by the AEI, before and after the $\mathcal{F}$-statistic correction.

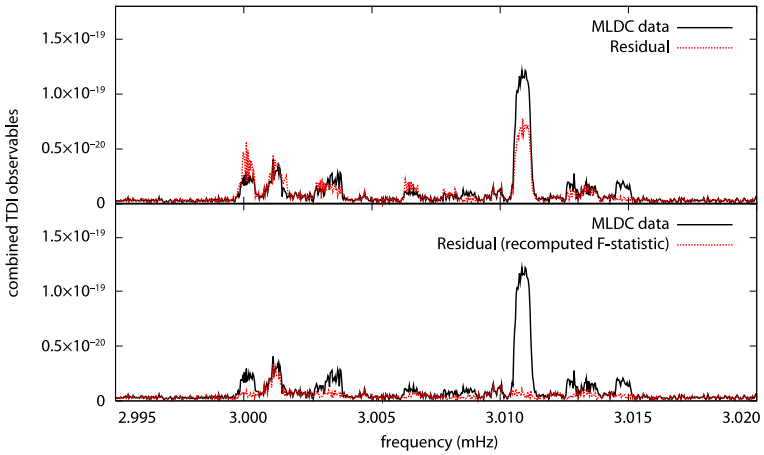

Figure 2. Plot of the amplitude of the signal in MLDC 1b.1.4 and the residual after subtracting the signal from the AEI entry, before and after the $\mathcal{F}$-statistic correction.

Table 4. The performance of challenge entries on the mildly confused binaries challenge as calculated using SNR, and C. Data in which the extrinsic parameters were corrected using the $\mathcal{F}$-statistic are denoted with an asterisk (*).

Group	SNR	C	# Recovered	False Positives
Challenge 1B.1.4 ($\mathrm{SNR}_{\mathrm{key}} = 340.233$, 51 Sources)				
AEI	375.366	0.774	13	2
AEI*	329.344	0.966	13	2
GSFC	209.411	0.003	6	1
GSFC*	90.506	0.282	6	1

Table 5. The performance of challenge entries on the highly confused binaries challenge as calculated using SNR, and C. Data in which the extrinsic parameters were corrected using the $\mathcal{F}$-statistic are denoted with an asterisk (*).

Group	SNR	C	# Recovered	False Positives
Challenge 1B.1.5 ($\mathrm{SNR}_{\mathrm{key}} = 273.206$, 44 Sources)				
AEI	208.273	0.453	3	0
AEI*	251.985	0.929	3	0

2.2. Massive Black Hole Binary Systems: Challenges 1B.2.X

Two data sets were released each containing a single and loud in-spiral signal from a MHB binary embedded in Gaussian and stationary noise; as in all the challenges so far, the in-spiral waveform was approximated at the restricted post^2-Newtonian order and the black holes were assumed to be non-spinning and in a circular orbit (see Section 3 for the important difference in the waveform model introduced in Challenge 3). Nine parameters described the waveform: the two masses $m_{1,2}$, the time to coalescence of the binary t_c, the sky position (β, λ), the luminosity distance D_L, the orbital inclination angle ι, the gravitational polarization angle ψ and the initial gravitational wave phase φ_0. The prior range, known to the Challenge participants, from which

the signals were drawn was $m_1 = 1 - 5 \times 10^6\, M_\odot$, $m_1/m_2 = 1 - 4$ and the time to coalescence $t_c = 6 \pm 1$ months and 400 ± 40 days for Challenge 1B.2.1 and Challenge 1B.2.2, respectively. All the other parameters were selected randomly from the full range.

Two groups submitted results for the massive black hole search. A collaboration of JPL scientists (that tackled both data sets) employed a three step hierarchical strategy combining a time-frequency track search analysis, followed by a template bank matched filter search, and a final stage based on a Metropolis-Hastings Monte Carlo technique to evaluate of posterior density functions of the model parameters. A group from Cardiff University used a stochastic template bank matched filter search[11] to analyse the Challenge 1B.2.1 data set. The results of the analyses are summarised in Table 6. The recovered SNR associated to the estimate of the parameters is very close to $SNR_{\rm key}$, which provide reassurance on the success of the analysis. However closer inspection of the errors on the individual parameters, in particular sky position β and λ, shows large discrepancies. In fact for Challenge 1B.2.1, both JPL and Cardiff analyses converged on secondary maxima of the likelihood function, very close in value to the true mode (as shown by the recovered SNR), but far in some of the parameters from the actual source parameters. In fact the JPL result places the source at almost at the antipodal sky position, while still recovering the SNR to better than one part in a thousand. This is a genuine result, which shows the benefit of actual analyses on mock data, compared to simple studies of the variance-covariance matrix that cannot uncover these subtleties. The specific results of Challenge 1B.2.1 have important repercussions for astronomy, *e.g.* in follow-ups of LISA-identified sources with other telescopes and call therefore for . It would however be an error to draw conclusive statements about the LISA ability of identifying MBH binaries in the sky: the waveforms used so far in MLDCs include simplifications, such as lack of spins and higher order harmonics in the amplitude that are known to break degeneracy amongst parameters. Challenge 3 MBH binaries waveforms will include the effect of spins, see next Section, and the results of the analyses will provide a more realistic insight into such issues.

2.3. Extreme Mass Ratio Inspirals: Challenges 1B.3.X

Searches for EMRIs were only partially attempted for Challenge 2 due to the complexity of an even basic end-to-end analysis pipeline. EMRIs data sets in Challenge 1B – five of them each containing a single EMRI superimposed to Gaussian and stationary noise with combined optimal SNRs between ≈ 55 and 135 and a range of source parameters, see [4] for details – represented the first real test-bed for analysis algorithms developed for this critical source class. Three groups – here identified by EtfAG, BBGP and MT2 – involving scientists at the AEI, Caltech, Cambridge University, Montana State University, University of Southampton and the University of Western Australia submitted entries for this challenge. EftAG employed a time-frequency technique [12], whereas BBGP and MT2 developed coherent approaches based on Monte Carlo techniques that differed in implementation (NEED GWDAW REF). The results were assessed using the criteria described in the introduction, although the EtfAG time-frequency analysis is insensitive to extrinsic parameters and the correlation and recovered SNR could not be computed. A summary of the results is given in Tables 7, 8.

Overall the results of this exercise were positive and provide a tangible proof that

Table 6. Relative/absolute errors for the MBH binaries in Challenges 1B.2.1 and 1B.2.2. Error estimates have been adjusted for degeneracies when certain symmetries are taken into account. In Challenge 1B.2.1, the error values for the polarization angle are given using the symmetry $\psi \to \psi + \pi$. In Challenge 1B.2.2, the error values for both ψ and φ_0 are due to the symmetries $\psi \to \psi + \pi/2$ and $\varphi_0 \to \varphi_0 - \pi/2$.

Challenge	1B.2.1		1B.2.2
$\mathrm{SNR}_{\mathrm{key}}$	531.84		80.67
Group	JPL	Cardiff	JPL
SNR	531.57	511.78	79.86
$\Delta m_1/m_1$	5.991×10^{-3}	0.108	0.122
$\Delta m_2/m_2$	-5.252×10^{-3}	-0.111	-0.134
$\Delta t_c/t_c$	1.369×10^{-5}	-3.601×10^{-5}	-7.296×10^{-5}
$\Delta D_L/D_L$	-0.139	-1.438	4.781×10^{-3}
$\Delta\beta$	2.429	1.374	5.862×10^{-3}
$\Delta\lambda$	3.133	0.548	-1.461×10^{-2}
$\Delta\iota$	0.713	0.678	-6.955×10^{-2}
$\Delta\psi$	-0.564	1.448	-4.878×10^{-2}
$\Delta\varphi_0$	-2.846	-2.389	-1.584

such complex problem is being successfully tackled. In fact, at least two radically different techniques are being pursued, both of which perform well on present MLDC data sets; all the EMRIs were detected, although only two groups analysed each data set and there was a spread of performance of the same analysis pipeline depending on the data set; somewhat poorer performances of selected analyses were due to lack of computational time before the deadline for submission and/or issues that were well understood but could not be resolved in time. It is worth highlighting some of the exquisite results for Challenge 1B.3.1, that seem to confirm (although in a simplified scenario) that LISA could indeed provide measurements of MBH parameters with unprecedented accuracy. It is also interesting to notice that for this specific type of data sets time-frequency techniques performed quite well.

Because the signals used in this challenge were quite strong, they could be relatively easy detected, as it was already shown in the challenge 1.3. The main achievement in the challenge 1B.3 as compared to 1.3, is the parameter estimation of the detected signals, as it is obvious from the Table 7 (especially MT2 entry for 1B.3.1). The techniques were significantly improved and they allowed to identify the secondary maxima, some results were submitted as "the best available" by the deadline, even though the groups have realized that this is not yet the true answer.

We caution the reader that general conclusions about the relative merit of analyses approaches and/or the overall quality of LISA astronomy for EMRIs would be inappropriate: it is not known as yet how these techniques scale as the SNR decreases – and this will begin to be addressed by Challenge 3 – and in situations in which EMRIs overlap a with large number of galactic binary signals and possibly with each other.

From this early development work and analysis results it is clearly emerging that the main challenge for (isolated) EMRI analyses is to deal with a very complex structure of the parameter space that produces a number of secondary maxima of the likelihood function with fairly similar values but well separated in parameter space. A similar issue was discussed for the MBH binary analyses.

Table 7. Errors for challenge 1.3.X.

Entry	$\frac{d\beta}{\Delta\beta}$	$\frac{d\lambda}{\Delta\lambda}$	$\frac{d\theta_K}{\Delta\theta_K}$	$\frac{d\phi_K}{\Delta\phi_K}$	$\frac{da}{\Delta a}$	$\frac{d\mu}{\Delta\mu}$	$\frac{dM}{\Delta M}$	$\frac{d\nu_0}{\nu_0}$	$\frac{de_0}{0.15}$	$\frac{d\lambda_{SL}}{\Delta\lambda_{SL}}$
BBGP-1B.3.1	-0.03	-0.0059	-0.14	0.053	0.31	-0.20	-0.84	0.026	0.37	-0.022
EtfAG-1B.3.1	0.019	-0.0045	0.56	0.33	0.16	-0.11	-0.27	-9.3e-05	0.17	0.078
MT2-1B.3.1	0.0058	0.0027	0.00044	0.0051	-0.0022	0.0065	0.014	3.2e-06	-0.0085	-0.0020
BBGP-1B.3.2	-0.16	-0.43	0.46	-0.33	-0.0088	-0.0040	0.016	0.00014	-0.010	-0.0013
EtfAG-1B.3.2	-0.014	0.0042	0.97	-0.36	0.0043	-0.046	-0.069	-6.5e-05	0.041	0.0041
MT2-1B.3.2	0.0040	-0.0086	0.79	0.41	0.093	-0.064	0.35	-0.035	0.068	0.092
BBGP-1B.3.3	0.091	0.50	-0.23	0.045	-0.32	-0.49	-0.029	0.00061	0.019	0.054
EtfAG-1B.3.3	-0.01	-0.004	0.49	-0.34	0.0073	-0.059	-0.061	-7.8e-05	0.038	0.0061
MT2-1B.3.3	0.045	-0.019	-0.1	0.077	-0.066	0.13	0.59	0.00036	-0.33	0.010
BBGP-1B.3.4	-0.57	-0.37	0.37	-0.31	-0.025	0.020	-0.88	0.066	0.065	-0.16
EtfAG-1B.3.4	-0.56	0.49	0.56	-0.34	0.059	0.12	0.04	0.00028	-0.039	0.0040
BBGP-1B.3.5	-0.48	-0.14	-0.35	0.1	-0.094	-0.094	0.55	-0.0021	-0.017	-0.060
EtfAG-1B.3.5	-0.58	0.46	0.27	-0.084	0.20	-0.7	0.83	-0.066	0.066	0.27

Table 8. The overlaps and recovered SNRs for the TDI channels A, E and the combined recovered SNR for Challenge 1.3.X. Entries labelled with (a) and (b) have been corrected for the sign of the latitude and the reference phases at $t = 0$, respectively.

Entry	overlap (A)	SNR_A	overlap (E)	SNR_E	SNR
					($\mathrm{SNR}_{\mathrm{key}} = 123.7$)
BBGP-1B.3.1	0.57	51 .0	0.58	51.6	72.5
MT2-1B.3.1	0.998	86.1	0.997	88.3	123.4
					($\mathrm{SNR}_{\mathrm{key}} = 133.5$)
BBGP-1B.3.2	0.07	6.6	0.18	18.2	17.6
BBGP-1B.3.2[a]	0.39	37.6	0.41	39.8	54.7
MT2-1B.3.2	0.54	49.5	0.54	50.8	70.9
					($\mathrm{SNR}_{\mathrm{key}} = 81.0$)
BBGP-1B.3.3	-0.06	-4.2	-0.0003	-0.05	-3.0
BBGP-1B.3.3[a]	-0.2	-11.5	-0.32	-19.0	-21.5
MT2-1B.3.3	22.0	22.0	20.5	20.9	30.4
					($\mathrm{SNR}_{\mathrm{key}} = 104.5$)
BBGP-1B.3.4	0.0007	2.1	-0.0002	0.8	2.1
BBGP-1B.3.4[b]	0.16	13.9	0.04	6.7	14.6
					($\mathrm{SNR}_{\mathrm{key}} = 57.6$)
BBGP-1B.3.5	0.09	3.4	0.1	4.2	5.3

3. Synopsis of Challenge 3

The third round of the MLDCs consists of five challenges (3.1–3.5):

- *Data set 3.1* contains a Galactic GW foreground from $\sim$ 60 million compact binary systems. This data set is a direct descendant of Challenge 2.1, but it improves on the realism of the latter by including both detached and interacting binaries with intrinsic frequency drifts (either positive or negative). Section 3.1 gives details about the binary waveform models, about their implementation in the LISAtools suite [13], and about the generation of the Galactic population.
- *Data set 3.2* contains GW signals from 4–6 binaries of spinning massive black holes (MBHs), on top of a confusion Galactic-binary background. This data set improves on the realism of Challenges 1.2.1–2 and 2.2 by modeling the orbital precession (and ensuing GW modulations) due to spin–orbit and spin–

spin interactions. Section 3.2 gives details about the MBH-binary waveforms. Because this challenge focuses on the effects of spins rather than on the joint search for MBH signals and for the brightest Galactic binaries, the background is already *partially subtracted*—it is generated from the population of detached binaries used for Challenge 3.1, withholding all signals with SNR > 5.

- *Data set 3.3* contains five GW signals from extreme–mass-ratio inspirals (EMRIs). As in Challenges 1.3.1–5, EMRI waveforms are modeled with Barack and Cutler's "analytic kludge" waveforms [14]; this challenge introduces the complication of detecting five such signals with lower SNRs, and *in the same data set*. By contrast, Galactic confusion is not included. See section 3.3 for details.

Data sets 3.1–3 consist of approximately two years of data (2^{22} samples at a cadence of 15 s) for time-delay interferometry (TDI) observables X, Y, and Z. These data sets are released both as time series of equivalent strain generated by the LISA Simulator [15] and as time series of fractional frequency fluctuations generated by Synthetic LISA [16]; see [4, p. S556] for the conversion between the two. Indeed (with a few exceptions, described below, for 3.4 and 3.5), the Challenge-3 data sets are built using the "pseudo-LISA" model of Challenges 1 and 2: the orbits of the LISA spacecraft are e^2-accurate Keplerian ellipses with conventional orientations and time offsets; *modified* TDI (a.k.a. TDI 1.5) expressions are used for the observables; and Gaussian, stationary instrument noise is included from six proof masses and six optical benches with known noise levels that are identical across each set of six.‡ See [4] for details.

Challenges 3.4 and 3.5 address the detection of two GW sources that are *new* to the MLDCs, and that have (respectively) bursty and stochastic characters: thus, these searches require an accurate characterization of instrument noise, which in reality will not be available *a priori*, but will be obtained from the LISA measurements themselves. To model this problem, in data sets 3.4 and 3.5 the levels of the six + six secondary noises have been independently randomized by $\pm 20\%$ (the noises are however still uncorrelated). In addition, these data sets contain time series for all twelve "raw" LISA phase measurements y_{ijk} and z_{ijk} [16], so that contestants may now build additional TDI observables to help characterize instrument noise. The phase measurements *do* include laser phase noise, because otherwise they would convey extra information unavailable from the real LISA; but laser noise is reduced in level to $\sim$ ten times the secondary noise at 1 mHz, so that it can be canceled relatively easily with TDI 1.5 implemented with moderate timing precision. To wit:

- *Data set 3.4* consists of 2^{21} samples at a cadence of 1 s ($\sim$ 24 days), and it contains GW burst signals from cosmic string cusps, occurring as a Poissonian

‡ The six proof-mass noises are uncorrelated and white in acceleration, with one-sided power spectral density (PSD)

$$S_{\rm acc}^{1/2}(f) = 3 \times 10^{-15} [1 + (10^{-4}\,{\rm Hz}/f)^2]^{1/2}\,{\rm m\,s^{-2}\,Hz^{-1/2}};$$

the six optical-path noises are uncorrelated and white in phase with with PSD

$$S_{\rm opt}^{1/2}(f) = 20 \times 10^{-12}\,{\rm m\,Hz^{-1/2}};$$

[Neil: insert conversion to LISA Simulator values?] the conversion to Synthetic LISA's dimensionless fractional frequency fluctuations is described on [16, p. 6]; the values actually used in the MLDCs are

$$S_{\rm acc}(f) = 2.5 \times 10^{-48} (f/{\rm Hz})^{-2} [1 + (10^{-4}\,{\rm Hz}/f)^2]\,{\rm Hz^{-1}};$$
$$S_{\rm opt}(f) = 1.8 \times 10^{-37} (f/{\rm Hz})^2\,{\rm Hz^{-1}}.$$

random process throughout the data set, with a mean of five events. Details about the waveforms are given in section 3.4. The data set is provided only as fractional frequency fluctuations generated by Synthetic LISA.

- *Data set 3.5* consists of 2^{20} samples at a cadence of 2 s (again $\sim$ 24 days), and it contains a stochastic GW background, which is isotropic, unpolarized, Gaussian and stationary; its spectrum grows at low frequencies as $1/f^3$, and its magnitude is set to a few times the secondary noise over a broad range of frequencies. Details about the synthesis of the background and the simpler model of the LISA orbits used for this challenge are given in section 3.5. The data set is provided as fractional frequency fluctuations generated by Synthetic LISA and by the new LISA simulator LISACode [17], recently integrated into the LISAtools suite [13]; thus, cross checks are possible between the two simulators.

LISACode [17] was developed at APC-Paris with the purpose of accurately mapping the impact of the different LISA subsystems on its science observations, and of bridging the gap between the basic principles of the LISA measurement and a future, more sophisticated end-to-end simulator. Thus, LISACode includes realistic representations of most of the ingredients that will influence LISA's sensitivity (such as orbits, instrument noise, Ultra Stable Oscillator time stamps, phasemeter response functions), internal generators for several gravitational waveforms (monochromatic and chirping binaries, stochastic backgrounds, etc.), as well as the construction of various TDI combinations. Many user-defined parameters make it possible to study the impact of different LISA configurations on its sensitivity. LISACode's conventions follow closely those of the MLDCs and of Synthetic LISA.

All the Challenge-3 data sets can be downloaded at `astrogravs.nasa.gov/docs/mldc/round3/datasets.html`, encoded in lisaXML [2], an XML-based format that can be displayed directly in modern web browsers, and handled easily in C/C++, Python, and MATLAB with the LISAtools I/O libraries [13]. Each data set is released in the blind challenge version and in a training version that includes the source parameters used to generate it. Additional training data sets can be generated easily with the LISAtools suite.§

The remainder of this section describes the GW signal models adopted for each data set. See [4] for the conversion of the GW polarizations in source frame (given here) to the LISA frame. Table 9 is a glossary of source parameters with their symbols and lisaXML descriptors, while table 10 is a summary of the GW content of each data set along with the ranges used to choose source parameters randomly.

[Verify definition of SNR?]

3.1. Chirping Galactic binaries

Data set 3.1 contains GWs from a population of $\sim 26 \times 10^6$ detached and $\sim 34 \times 10^6$ interacting Galactic binaries. Each binary is modelled as a system of two point masses m_1 and m_2 in circular orbit with linearly increasing or decreasing frequency (depending on whether gravitational radiation or equilibrium mass transfer is dominant). The polarization amplitudes at the Solar-system barycenter, expressed in the source frame,

§ After installing LISAtools following the instructions at `code.google.com/p/lisatools/wiki/Install`, generating a training set is as simple as running (say, for Challenge 3.1)

```
MLDCpipelines2/bin/challenge3.py -T -R 3.1
```

Table 9. Source parameters in Challenge 3. We do not deal explicitly with the redshifting of sources at cosmological distances; thus, D is a *luminosity* distance, and all masses and frequencies are those measured at the SSB, which are red/blue-shifted by factors $(1+z)^{\pm 1}$ with respect to those measured locally near the sources.

Parameter	Symbol	Standard parameter name (lisaXML descriptor)	Standard unit (lisaXML descr.)
		Common parameters	
Ecliptic latitude	β	`EclipticLatitude`	`Radian`
Ecliptic longitude	λ	`EclipticLongitude`	`Radian`
Polarization angle	ψ	`Polarization`	`Radian`
Inclination	ι	`Inclination`	`Radian`
Luminosity distance[a]	D	`Distance`	`Parsec`
		Galactic binaries	
Amplitude[b]	$\mathcal{A}$	`Amplitude`	`1` (GW strain)
Frequency	f	`Frequency`	`Hertz`
Frequency derivative	$\dot{f}$	`FrequencyDerivative`	`Hertz/Second`
Initial GW phase	ϕ_0	`InitialPhase`	`Radian`
		Spinning massive black-hole binaries	
Masses of component MBHs	m_1, m_2	`Mass1`, `Mass2`	`SolarMass`
Magnitude of spins S_1, S_2	a_1, a_2	`Spin1`, `Spin2`	`MassSquared`
Initial orientation of spin S_1	θ_{S1}, ϕ_{S1}	`PolarAngleOfSpin1`	`Radian`
		`AzimuthalAngleOfSpin1`	`Radian`
Initial orientation of spin S_2	θ_{S2}, ϕ_{S2}	*... likewise*	
Time to coalescence	T_c	`CoalescenceTime`	`Second`
Phase at coalescence	Φ_c	`PhaseAtCoalescence`	`Radian`
Initial orientation	θ_L, ϕ_L	`InitialPolarAngleL`	`Radian`
of orbital momentum		`InitialAzimuthalAngleL`	`Radian`
		EMRIs: see table 5 of [4]	
		Cosmic string cusp bursts	
Amplitude[b] (Fourier)	$\mathcal{A}$	`Amplitude`	`Hertz^(1/3)`
Central time of arrival	t_C	`CentralTime`	`Second`
Maximum frequency[c]	$f_{\max}$	`MaximumFrequency`	`Hertz`
		Isotropic stochastic background	
PSD[b,d] at 1 Hz	S_h	`PowerSpectralDensity`	`(f/Hz)^-3/Hz`

[a] We do not deal explicitly with the redshifting of sources at cosmological distances, so D is a *luminosity* distance, and all masses and frequencies are measured at the SSB and red/blue-shifted by factors $(1+z)^{\pm 1}$ with respect to those measured locally near the sources.
[b] Replaces D for Galactic binaries, cosmic-string–cusp bursts, and stochastic-background pseudosources.
[c] Effectively replaces ι for cosmic-string–cusp bursts.
[d] Also: $S_h = S_h^{\rm tot}/384$; ψ is set to 0, and ι not used.

Table 10. Summary of data-set content and source-parameter selection in Challenge 3. Parameters are sampled randomly from uniform distributions across the ranges given below, and all angular parameters (including spin and orbital–angular-momentum directions for MBH binaries) are drawn randomly from uniform distributions over the whole appropriate ranges. Source distances are set from individual-source SNRs, which are drawn randomly from the ranges specified below (in Challenge 3, "SNR" refers to the multiple–TDI-observable SNR approximated as $\sqrt{2} \times \max\{\mathrm{SNR}_X, \mathrm{SNR}_Y, \mathrm{SNR}_Z\}$). The MBH time of coalescence t_c and the cosmic-string–cusp burst central time t_C are given relative to the beginning of the relevant data sets.

Dataset	Sources	Parameters
3.1	*Galactic-binary background*	randomized population (see section 3.1) $\sim 34 \times 10^6$ interacting, $\sim 26 \times 10^6$ detached
	plus 20 *verification binaries*	known parameters (see section 3.1)
3.2	4–6 *MBH binaries*	for each: $m_1 = 1$–$5 \times 10^6\, M_\odot$, $m_1/m_2 = 1$–4, $a_1/m_1 = 0$–1, $a_2/m_2 = 0$–1
	... including	MBH$_1$: $t_c = 90 \pm 30$ days, SNR ~ 2000 MBH$_2$: $t_c = 765 \pm 15$ days, SNR ~ 20
	... and 2–4 chosen from	MBH$_3$: $t_c = 450 \pm 270$ days, SNR ~ 1000 MBH$_4$: $t_c = 450 \pm 270$ days, SNR ~ 200 MBH$_5$: $t_c = 540 \pm 45$ days, SNR ~ 100 MBH$_6$: $t_c = 825 \pm 15$ days, SNR ~ 10
	plus *Galactic confusion*	randomized population with approx. SNR < 5 $\sim 26 \times 10^6$ binaries; no verification
3.3	5 *EMRIs*	for each: $\mu = 9.5$–$10.5\, M_\odot$, $S = 0.5$–$0.7\, M^2$, time at plunge $= 2^{21}$–$2^{22} \times 15$ s, ecc. at plunge $= 0.15$–0.25, SNR $= 10$–50
	... including	EMRI$_1$: $M = 0.95$–$1.05 \times 10^7 M_\odot$ EMRI$_2$ and EMRI$_3$: $M = 4.75$–$5.25 \times 10^6 M_\odot$ EMRI$_4$ and EMRI$_5$: $M = 0.95$–$1.05 \times 10^6 M_\odot$
3.4	*n Cosmic-string–cusp bursts*	(with n Poisson-distributed with mean 5) $f_{\max} = 10^{-3-1}$ Hz, $t_C = 0$–2^{21} s, SNR $= 10$–100 all instrument noise levels randomized ±20%
3.5	*Isotropic stochastic background*	2×192 incoherent h_+ and $h_\times$ sources over sky $S_h^{\mathrm{tot}} = 0.7$–$1.3 \times 10^{-47} (f/\mathrm{Hz})^{-3}\,\mathrm{Hz}^{-1}$ all instrument noise levels randomized ±20%

are given by

$$h_+^S(t) = \mathcal{A}\left(1 + \cos^2\iota\right)\cos[2\pi(ft + \dot{f}t^2/2) + \phi_0], \qquad (4)$$
$$h_\times^S(t) = -2\mathcal{A}(\cos\iota)\sin[2\pi(ft + \dot{f}t^2/2) + \phi_0],$$

where the amplitude is derived from the physical parameters of the source as $\mathcal{A} = (2\mu/D)(\pi M f)^{2/3}$, with $M = m_1 + m_2$ the total mass, $\mu = m_1 m_2/M$ the reduced mass, and D the distance; $\dot{f}$ is the (constant) frequency derivative, and ϕ_0 is the phase at $t = 0$.

Since it would be unfeasible to process millions of barycentric binary waveforms individually through the LISA simulators to compute the TDI-observable time

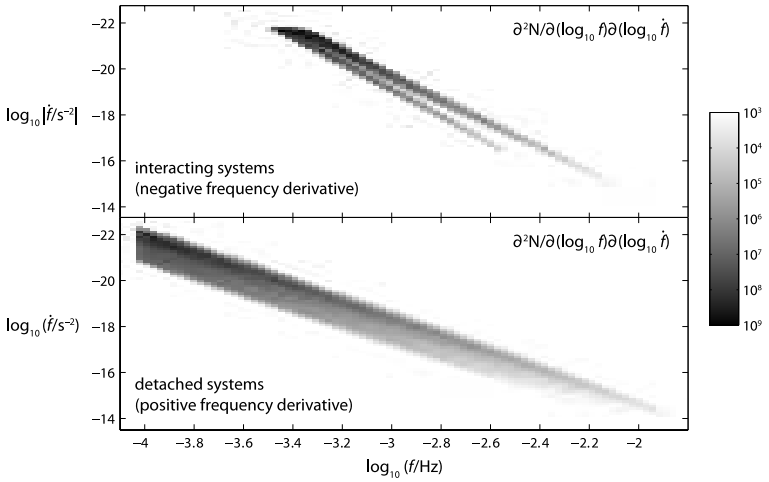

Figure 3. Histogram of the density of Galactic binaries in the Nelemans catalogs, binned by $\log_{10} f$ and $\log_{10} \dot{f}$.

series, we adopt a fast frequency-domain method [18] that rewrites the LISA phase measurements as the fast–slow decomposition

$$y_{ij}(t) = C(t)\cos(2\pi f_0 t) + S(t)\sin(2\pi f_0 t) \tag{5}$$

the functions $C(t)$ and $S(t)$ describe slowly varying effects such as the rotation of the LISA arms, the Doppler shift induced by orbital motion, and the intrinsic frequency evolution of the source. These "slow" terms can be sampled very sparsely and Fourier-transformed numerically, while the "fast" sine and cosine terms can be Fourier-transformed analytically. The results are then convolved to produce the LISA phase measurements, and these are assembled into the desired TDI variables. This algorithm is three to four orders of magnitude faster than the time-domain LISA simulators, although it effectively approximates LISA as a rigidly rotating triangle with equal and constant armlengths. See [18] for full details, and `lisatools/MLDCwaveforms/Galaxy3` for the source code.

The starting point for each realization of data set 3.1 are two large catalogs provided by Gijs Nelemans (files `MLDCwaveforms/Galaxy3/Data/AMCVn_GWR_MLDC.dat` and `dwd_GWR_MLDC.dat` in the LISAtools installation), which contain the parameters of 26.1×10^6 detached and 34.2×10^6 interacting systems produced by the population synthesis codes described in [19, 20]. Figure 3 shows the distribution of the binaries in the catalogs over f and $\dot{f}$. Recent work by Roelofs, Nelemans and Groot [21] suggests that the model in [20] overpredicts the number of (AM CVn) interacting systems by a factor of 5–10, but we did not implement this correction for Challenge 3.

The parameters of each binary in the catalogs are modified by randomly tweaking f by $\pm 1\%$, A by $\pm 10\%$, β and λ by $\pm 0.5\,^\circ$, and by randomly assigning ψ, ι, and ϕ_0 ($\dot{f}$ is computed from the catalog's binary-period derivative and from the tweaked f). These random perturbations are large enough to render the original population files useless as answer keys, but small enough to preserve the overall parameter distributions. Binaries with approximate single-Michelson SNR > 10 are regarded as "bright" and listed in a separate table in the challenge keys. Data set 3.1

includes also 20 verification binaries of known parameters (specified in LISAtools file `MLDCwaveforms/Galaxy3/Data/Verification.dat` as rows of f, $\dot{f}$, β, λ, A).

3.2. Spinning MBH binaries

The spinning-MBH binary GW signals of data set 3.2 are modeled as 2PN circular adiabatic inspirals with uncoupled orbital frequency evolution and spin and orbital precession. No higher-PN harmonics are included. Both phase and orbital frequency are explicit functions of time (TaylorT3 in classification presented in [22]):

$$M\omega = \frac{1}{8}\tau^{-3/8}\left[1+\left(\frac{743}{2688}+\frac{11}{32}\eta\right)\tau^{-1/4}-\frac{3}{10}\left(\pi-\frac{\beta}{4}\right)\tau^{-3/8}+\right.$$
$$\left.+\ \left(\frac{1855099}{14450688}+\frac{56975}{258048}\eta+\frac{371}{2048}\eta^2-\frac{3}{64}\sigma\right)\tau^{-1/2}\right] \tag{6}$$

where $\eta = \mu/M$ is symmetric mass ratio and

$$\tau = \frac{\eta}{5M}(T_c - t), \tag{7}$$

$$\beta = \frac{1}{12}\sum_{i=1,2}\left[\chi_i\left(\hat{\mathbf{L}}_\mathbf{N}.\hat{\mathbf{S}}_\mathbf{i}\right)\left(113\frac{m_i^2}{M^2}+75\eta\right)\right] \tag{8}$$

$$\sigma = -\frac{1}{48}\eta\chi_1\chi_2\left[247(\hat{\mathbf{S}}_\mathbf{1}.\hat{\mathbf{S}}_\mathbf{2})-721(\hat{\mathbf{L}}_\mathbf{N}.\hat{\mathbf{S}}_\mathbf{1})(\hat{\mathbf{L}}_\mathbf{N}.\hat{\mathbf{S}}_\mathbf{2})\right] \tag{9}$$

Here $\hat{\mathbf{L}}_\mathbf{N}$, $\hat{\mathbf{S}}_1$, $\hat{\mathbf{S}}_2$ are unit vectors along leading order angular orbital momentum and hole's spins. The intrinsic orbital phase is

$$\Phi_{orb} = \Phi_C - \frac{\tau^{5/8}}{\eta}\left[1+\left(\frac{3715}{8064}+\frac{55}{96}\eta\right)\tau^{-1/4}-\frac{3}{16}(4\pi-\beta)+\right.$$
$$\left.\left(\frac{9275495}{14450688}+\frac{284875}{258048}\eta+\frac{1855}{2048}\eta^2-\frac{15}{64}\sigma\right)\tau^{-1/2}\right]. \tag{10}$$

Due to the spin-orbital coupling the spins and orbital angular momentum are precessing around total angular momentum, therefor we need to add precessional correction to the orbital phase (see [23]):

$$\dot{\Phi} = \omega + \frac{(\hat{\mathbf{L}}_\mathbf{N}.\hat{\mathbf{n}})[\hat{\mathbf{L}}_\mathbf{N}\times\hat{\mathbf{n}}]\dot{\hat{\mathbf{L}}}_N}{1-(\hat{\mathbf{L}}_\mathbf{N}.\hat{\mathbf{n}})^2} \equiv \omega + \delta\dot{\Phi}, \tag{11}$$

where $\hat{\mathbf{n}}$ is direction to the source in SSB. The constant of integration of (11), Φ_C, can be redefined so that $\delta\dot{\Phi} = 0$ at $t = 0$. The precession equations for $\hat{\mathbf{L}}_\mathbf{N}$, $\hat{\mathbf{S}}_1$, $\hat{\mathbf{S}}_2$ are given by eqn. (2.9)-(2.11) in [24]. As mentioned above we use restricted waveform (only leading order amplitude) and in the source frame (with the phasing formulae above) it takes the following form

$$h_+ = -2\frac{\mu}{D}(1+\cos(i)^2)(M\omega)^{2/3}\cos 2\Phi \tag{12}$$

$$h_\times = 4\frac{\mu}{D}\cos(i)(M\omega)^{2/3}\sin 2\Phi. \tag{13}$$

The inclination angle i is defined by initial position of the orbital momentum and by the direction to the source: $\cos i = (\hat{\mathbf{L}}_\mathbf{N}.\hat{\mathbf{n}})$. Note that if one uses the approach given

in [25], the amplitudes will be more complicated and the precession part of the phase at $t = 0$ should be $\delta\dot{\Phi}^K = -\gamma^K$, where superscript K stands for Kidder and

$$\gamma^K = \frac{\mathbf{e}_z \times \hat{\mathbf{L}}_\mathbf{N}}{|\mathbf{e}_z \times \hat{\mathbf{L}}_\mathbf{N}|} \frac{\hat{\mathbf{L}}_\mathbf{N} \times \hat{\mathbf{n}}}{\sqrt{1 - (\hat{\mathbf{L}}_\mathbf{N}.\hat{\mathbf{n}})^2}}.$$

The end of the inspiral is handled with an exponential taper, as in Challenge 2. The expressions for h_+ and $h_\times$ are given in the time varying polarization basis, but to generate the LISA responses it is necessary to re-express it in terms of fixed polarization tensors. This is achieved through a rotation by the polarization angle ψ:

$$\tan\psi = \frac{\cos\beta\cos(\lambda - \phi_L)\sin\theta_L - \cos\theta_L\sin\beta}{\sin\beta\sin(\lambda - \phi_L)}. \tag{14}$$

and the waveform in SSB becomes

$$h_+^{\mathrm{SSB}} = -h_+\cos 2\psi - h_\times \sin 2\psi \tag{15}$$

$$h_\times^{\mathrm{SSB}} = h_+\sin 2\psi - h_\times\cos 2\psi. \tag{16}$$

Masses, SNRs, and times of coalescence are chosen as in Challenge 2 (see also table 10); the spin magnitudes S_1/M_1^2 and S_2/M_2^2 are drawn uniformly in $[0, 1]$; all the angles (spin directions, initial orbital angular momentum, sky position) are drawn uniformly over spheres. See `lisatools/MLDCwaveforms/FastBBH` for the source code.

Dataset 3.2 includes also a Galactic confusion background generated from the same detached-binary population as used in Challenge 3.1 (interacting systems have typically very small chirp masses and are not expected to make a significant contribution), but withholding all binaries with individual SNR > 5 relative to instrument noise **[Neil: is this right?]** The resulting confusion background is described well **[Neil: is this true?]** by the analytical PSD expression

$$S_{X,\mathrm{gal}} = 16\,x^2\sin^2 x\,\mathrm{Hz}^{-1} \times \begin{cases} 10^{-44.62}(f/\mathrm{Hz})^{-2.3} & \text{for } f \in [10^{-4}, 10^{-3}]\ \ \mathrm{Hz}, \\ 10^{-50.92}(f/\mathrm{Hz})^{-4.4} & \text{for } f \in [10^{-3}, 10^{-2.7}]\ \ \mathrm{Hz}, \\ 10^{-62.8}\ (f/\mathrm{Hz})^{-8.8} & \text{for } f \in [10^{-2.7}, 10^{-2.4}]\ \mathrm{Hz}, \\ 10^{-89.68}(f/\mathrm{Hz})^{-20.0} & \text{for } f \in [10^{-2.4}, 10^{-2.0}]\ \mathrm{Hz}, \end{cases} \tag{17}$$

(fractional frequency fluctuations, with $x = 2\pi f L$, $L \simeq 16.6782$ s), which was derived using a BIC criterion for the resolvability of individual Galactic binaries [18], and is used in Challenge 3 (on top of instrument noise) to define the SNRs of GW signals from MBH binaries, EMRIs (Challenge 3.3), and cosmic-string cusps (Challenge 3.4).

3.3. EMRIs

The EMRI waveforms of data set 3.3 are the Barack–Cutler [14] "analytic kludges" used for Challenge 1.3.1–5 and described in [4, sec. 4.5], with the single change in that the number of eccentric-orbit harmonics included in the waveform does not evolve with eccentricity, but is fixed at five (lisaXML parameter `FixHarmonics`; a value of zero will reproduce the old behavior). See `lisatools/MLDCwaveforms/EMRI` for the source code.

3.4. Cosmic string cusps

Data set 3.4 contains a number of bursts from cosmic strings, the first of two new GW sources introduced with Challenge 3. Cosmic strings are linear topological defects that may be formed in early Universe at the phase transitions predicted in many elementary-particle and superstring models. Cosmic-string oscillations emit gravitational radiation, with a substantial part of the emission from *cusps*, which can achieve very large Lorentz boosts [26]. In the limit where the tip of a cusp is moving directly toward the observer, the observed metric perturbation is a linearly polarized GW with [27]

$$h(t) = A|t - t_C|^{1/3}, \quad A \sim \frac{G\mu L^{2/3}}{D_L}; \tag{18}$$

here t_C is the burst's central time of arrival, G is Newton's constant, μ is the string's mass per unit length, D is the luminosity distance to the source, and L is the size of the feature that produces the cusp (e.g., the length of a cosmic string loop). If the observer's line of sight does not coincide with the cusp's direction of motion, the waveform becomes a much more complicated mixture of polarizations [28]. If the viewing angle α departs only slightly from zero, the waveform remains dominantly linearly polarized, and the sharp spike in (18) is rounded off, introducing an exponential suppression of Fourier-domain power for frequencies above $f_{\max} = 2/(\alpha^3 L)$.

Following the model used by the LIGO Science Collaboration, we define our cusp waveforms in the Fourier domain according to

$$|h_+(f)| = \mathcal{A} f^{-4/3} \left(1 + (f_{\rm low}/f)^2\right)^{-4}, \quad h_\times = 0, \tag{19}$$

with $\exp(1 - f/f_{\max})$ suppression above $f_{\max}$. The amplitude $\mathcal{A}$ has dimensions $\mathrm{Hz}^{1/3}$; $f_{\rm low}$ sets the low-frequency cut-off of what is effectively a fourth-order Butterworth filter, which prevents dynamic-range issues with the inverse Fourier transforms (for Challenge 3 we set $f_{\rm low} = 1 \times 10^{-5}$ Hz). The phase of the waveform is set to $\exp \mathrm{i}(\pi - 2\pi f t_C)$ before inverse-Fourier transforming to the time domain. See `lisatools/MLDCwaveforms/CosmicStringCusp` for the source code.

3.5. Stochastic background

Data set 3.5 contains the second GW source new to Challenge 3: an isotropic, unpolarized, Gaussian and stationary stochastic background. Allen and Romano [29] define a stochastic background as the "gravitational radiation produced by an extremely large number of weak, independent, and unresolved gravity-wave sources, [...] stochastic in the sense that it can be characterized only statistically." Such backgrounds are usually characterized by the dimensionless quantity

$$\Omega_{\rm gw}(f) = \frac{1}{\rho_{\rm crit}} \frac{\mathrm{d}\rho_{\rm gw}}{\mathrm{d}\log f}, \tag{20}$$

with $\rho_{\rm gw}$ the energy density in GWs, and $\rho_{\rm crit} = 3c^2 H_0^2/(8\pi G)$ the closure energy density of the Universe, and they are idealized as the collective, incoherent radiation of uncorrelated infinitesimal emitters distributed across the sky. If the background is isotropic, unpolarized, Gaussian and stationary, the Fourier amplitude $\tilde{h}_A(f, \hat{\Omega})$ of

each emitter (with A indexing the + and × polarizations, and $\hat{\Omega}$ the direction on the two sphere) is completely characterized by the power-spectral-density relation [29]

$$\left\langle \tilde{h}^*_A(f,\hat{\Omega})\tilde{h}_{A'}(f',\hat{\Omega}')\right\rangle = \frac{3H_0^2}{32\pi^3}|f|^{-3}\Omega_{\rm gw}(|f|)\times\delta_{AA'}\delta(f-f')\delta^2(\hat{\Omega},\hat{\Omega}'). \quad (21)$$

In Challenge 3, we assume a constant $\Omega_{\rm gw}(f)$, as appropriate for the primordial background predicted in many cosmological scenarios. We implement the uncorrelated emitters as a collection of 192 pseudosources distributed at *HEALPix* pixel centers across the sky. HEALPix (the Hierarchical Equal Area isoLatitude Pixelization of spherical surfaces [30]) is often used to represent cosmic microwave background data sets; 192 pixels correspond to a twice-refined HEALPix grid with $N_{\rm side} = 2^2$.

Each pseudosource consists of uncorrelated pseudorandom processes for h_+ and $h_\times$, generated as white noise in the time domain, and filtered to achieve the f^{-3} spectrum of (21), using the the recursive $1/f^2$ filtering algorithm proposed by Plaszczynski [31], extended to spectral slope -3. The algorithm employs a chain of $1/f^2$ infinite–impulse-response filters to reshape the white noise spectrum between minimum and maximum frequencies $f_{\rm low}$ and $f_{\rm knee}$, set to 10^{-5} and 10^{-2} Hz in this Challenge (see source code `lisatools/MLDCwaveforms/Stochastic.py` for the Synthetic LISA implementation).

The *one-sided* PSD of each single-polarization random process (which represents the finite area of a pixel in the sky) is then given by $S_h(f)/2 = 3H_0^2/(32\pi^3)f^{-3}\Omega_{\rm gw}\times(4\pi^2/192)$. In data set 3.5, we define $S_h^{\rm tot} = (192\times 2)S_h$ and we set it so that, in the TDI observables, the GW background is a few times stronger than LISA's secondary instrument noise. Namely,

$$S_h^{\rm tot}(f) = 0.7\text{–}1.3\times 10^{-47}(f/{\rm Hz})^{-3}\,{\rm Hz}^{-1} \quad (22)$$

(taking $H_0 = 70\,$km/s/Mpc, this corresponds to $\Omega_{\rm gw} = 8.95\times10^{-12}$–$1.66\times10^{-11}$). **[Check the 1/2 for the one-sided spectrum.]**

One of the more promising approaches to detect GW backgrounds with LISA relies on estimating instrument noise levels by way of symmetrized TDI observables that is insensitive to GWs at low frequencies in the LISA band [32]. For realistic LISA orbits, however, the low-frequency behavior of such observables becomes more complicated than discussed in the literature. To simplify the initial investigation of the background-detection problem in data set 3.5, we have therefore approximated LISA as a rigidly rotating triangle with equal and constant armlengths (i.e., Synthetic LISA's `CircularRotating`).

4. Conclusion

We are very excited about the outcome of the first two MLDCs, which have given a convincing demonstration that a significant portion of the LISA science objectives could already be achieved with techniques that are currently in hand. Most of the research groups that participated in Challenge 1 have successfully made the transition to the greater complexity of Challenge 2. Challenge 3 (with data sets released in Jan 2008 and results due in Dec 2008) will continue to move in the direction of more realistic signals, featuring chirping Galactic binaries and precessing binaries of spinning MBHs. It will also include two new classes of signals: an isotropic primordial GW background and bursts from the cusps of cosmic strings. In addition, Challenge 1B took place between July and Dec 2007. This was a repeat of Challenge 1, conceived to

provide a softer entry point for research groups new to the MLDCs. Ten collaborations (including five new institutions) participated, demonstrating increasing sophistication and proficiency in a range of LISA data-analysis techniques.

Furthermore, the MLDC conventions, file formats, and software tools [13] have matured to the point where interested parties can use them to generate a variety of data sets. This enables a wealth of interesting side investigations, such as the studies of the LISA science reach that are now being undertaken by the LISA Science Team. To obtain more information and to participate in the MLDCs, see the official MLDC website (`astrogravs.nasa.gov/docs/mldc`) and the task force wiki (`www.tapir.caltech.edu/listwg1b`). [**These two paragraphs are verbatim from the MLDC-2 report. Need to shorten, rephrase, add more about results.**]

Acknowledgments

SB and EP were supported by the Deutsches Zentrum für Luft- und Raumfahrt; LW's work by the Alexander von Humboldt Foundation's Sofja Kovalevskaja Programme funded by the German Federal Ministry of Education and Research. JG thanks the Royal Society for support and the Albert Einstein Institute for hospitality and support while part of this work was being completed. SF was supported by the Royal Society, BSS and IH by the UK Science and Technology Facilities Council. MV was supported by the LISA Mission Science Office and by JPL's HRDF. CC's, JC's and MV's work was carried out at the Jet Propulsion Laboratory, California Institute of Technology, under contract with the National Aeronautics and Space Administration. MT acknowledges support from the Spanish Ministerio de Eduación y Ciencia Research projects FPA-2007-60220, CSD207-00042 and the Govern de les Illes Balears, Conselleria d'Economia, Hisenda i Innovació. IM was partially supported by NASA ATP Grant NNX07AH22G to Northwestern University.

References

[1] Bender P, Danzmann P and the LISA Study Team 1998 "Laser Interferometer Space Antenna for the Detection of Gravitational Waves, Pre-Phase A Report" **MPQ 233** (Garching: Max-Planck-Institüt für Quantenoptik)

[2] Arnaud K A et al. (the MLDC Task Force) 2006 *Laser Interferometer Space Antenna: 6th International LISA Symp. (Greenbelt, MD, 19–23 Jun 2006)* ed Merkowitz S M and Livas J C (Melville, NY: AIP) p 619; *ibid.* p 625 (long version with lisaXML description: *Preprint* gr-qc/0609106)

[3] Arnaud K A et al. (the MLDC Task Force and Challenge 1 participants) 2007 *Class. Quant. Grav.* **24** S529

[4] Arnaud K A et al. (the MLDC Task Force) 2007 *Class. Quant. Grav.* **24** S551

[5] Babak S et al. (the MLDC Task Force and Challenge 2 Participants) 2007 proceedings of the 7th Amaldi Conference on Gravitational Waves (8–14 July 2007, Sydney, Australia) *Preprint* arXiv:0711.2667

[6] Xspec, an X-ray Spectral Fitting Package, `heasarc.gsfc.nasa.gov/docs/xanadu/xspec`

[7] Jaranowski P, Krolak A and Schutz B F 1998 *Phys. Rev. D* **58** 063001

[8] Prix R and Whelan J T 2007 *Class. Quant. Grav.* **24** S565; *Poster* `www.ligo.caltech.edu/docs/G/G070462-00.pdf`

[9] Trias M, Vecchio M and Veitch J 2008 "Markov Chain Monte Carlo searches for Galactic binaries in MLDC-1B data sets" in this volume

[10] Gijs Nelemans' LISA wiki, `www.astro.kun.nl/~nelemans/dokuwiki`

[11] Harry I, Fairhurst S and Sathyaprakash B S 2008 "A Search for Super Massive Black Hole Coalescences in the Mock LISA Data Challenges" in this volume

[12] Gair J R, Mandel I and Wen L "Improved time-frequency analysis of extreme-mass-ratio inspiral signals in mock LISA data" in this volume
[13] LISAtools website and SVN repository, `lisatools.googlecode.com`
[14] Barack L and Cutler C 2004 *Phys. Rev. D* **69** 082005
[15] Cornish N J and Rubbo L J 2003 *Phys. Rev. D* **67** 022001; erratum-ibid. 029905; LISA Simulator website, `www.physics.montana.edu/lisa`; now included in [13]
[16] Vallisneri M 2005 *Phys. Rev. D* **71**; Synthetic LISA website, `www.vallis.org/syntheticlisa`; now included in [13]
[17] Petiteau A, Auger G, Halloin H, Jeannin O, Plagnol E, Pireaux S, Regimbeau T and Vinet J–Y 2008 *Phys. Rev. D* **77** 023002; LISACode website, `www.apc.univ-paris7.fr/LISA-France/analyse.phtml`; now included in [13]
[18] Cornish N J and Littenberg T B 2007 *Phys. Rev. D* **76** 083006
[19] Nelemans G, Yungelson L R and Portegies Zwart S F 2001, *Astron. Astrophys.* **375** 890
[20] Nelemans G, Yungelson L R and Portegies Zwart S F 2004, *Mon. Not. Roy. Astron. Soc.* **349** 181
[21] Roelofs G H A, Nelemans G and Groot P J 2007 *Mon. Not. Roy. Astron. Soc.* **382** 685
[22] Damour T, Iyer B and Sathyaprakash B S 2001 *Phys. Rev. D* **63** 044023
[23] Apostolatos T A, Cutler C, Sussman G J and Thorne K S 1994 *Phys. Rev. D* **49** 6274
[24] Lang R N and Hughes S A 2006 *Phys. Rev. D* **74** 122001
[25] Kidder L E 1995 *Phys. Rev. D* **52** 821
[26] Damour T and Vilenkin A 2000 *Phys. Rev. Lett.* **85** 3761
[27] Siemens X, Creighton J, Maor I, Ray Majumder S, Cannon K and Read J 2006 *Phys. Rev. D* **73** 105001
[28] Siemens X and Olum K D 2003 *Phys. Rev. D* **68** 085017
[29] Allen B and Romano J D 1999 *Phys. Rev. D* **59** 102001
[30] Górski K M et al. 2005 *Astrophys. J.* **622** 759; HEALPix website, `healpix.jpl.nasa.gov`
[31] Plaszczynski S 2007 *Fluctuation Noise Lett.* **7** R1
[32] Tinto M, Armstrong J W and Estabrook F B 2000 *Phys. Rev. D* **63** 021101